Applied Microscopy
Korean Society of Microscopy

pISSN 2287-5123 · eISSN 2287-4445
http://dx.doi.org/10.9729/AM.2012.42.4.179

Ultrastructural Abnormalities in APP/PSEN1 Transgenic Mouse Brain as the Alzheimer's Disease Model

Mi Jeong Kim†, Yang Hoon Huh†, Ki Ju Choi, Sangmi Jun, A Reum Je, Heesu Chae, Chulhyun Lee[1], Hee-Seok Kweon*

Division of Electron Microscopic Research, Korea Basic Science Institute, Daejeon 305-806, Korea
[1]Division of Magnetic Resonance Research, Korea Basic Science Institute, Chungbuk 363-883, Korea

Alzheimer's disease (AD) is a progressive neurodegenerative disorder. Neuropathological hallmarks of AD are amyloid plaques, dystrophic neurite, and alteration of subcellular organelles. However, the morpho-functional study of this degenerative process and ultimate neuronal death remains poorly elucidated. In this study, immunohistochemical and ultrastructural analyses were performed to clarify the abnormal morphological alterations caused by the progression of AD in APP/PSEN1 transgenic mice, express human amyloid precursor protein, as a model for AD. In transgenic AD mice brain, the accumulation of Amyloid β plaques and well-developed dystrophic neurites containing anti-LC3 antibody-positive autophagosomes were detected in the hippocampus and cortex regions. We also found severe disruption of mitochondrial cristae using high-voltage electron microscopy and three-dimensional electron tomography (3D tomography). These results provide morpho-functional evidence on the alteration of subcellular organelles in AD and may help in the investigation of the pathogenesis of AD.

Key Words: Alzheimer's diesese, Amyloid beta, Dystrophic neurite, High-voltage electron microscopy, Electron tomography

†These authors contributed equally to this work.

*Correspondence to:
Kweon HS,
Tel: +82-42-865-3685
Fax: +82-42-865-3939
E-mail: hskweon@kbsi.re.kr

Received October 27, 2012
Revised November 19, 2012
Accepted November 19, 2012

INTRODUCTION

Alzheimer's disease (AD) is a progressive neurodegenerative disorder that is the most common cause of dementia in the elderly. It is characterized by age-dependent decline of memory and multiple cognitive functions and severe neurodegeneration (Manczak et al., 2010). Various neurophathological hallmarks of AD are reported, such as intracellular neurofibrillary tangles, amyloid β (Aβ) plaque, dystrophic neurite, mitochondrial abnormalities, synapse loss, synaptic damage, and the loss of specific populations of neuron (Nixon et al., 2005; Manczak et al., 2006). Neurofibrillary tangles and Aβ plaques especially have been found in the hippocampus region of the brain, which is responsible for learning and memory in AD patient and AD transgenic mice (Reddy, 2009; Kocherhans et al., 2010). Amyloid peptide accumulations in the intracellular organelles, such as mitochondria (Manczak et al., 2006), synapse (Takahashi et al., 2004), Golgi apparatus (Stieber et al., 1996), and autophagosome (Nixon et al., 2005; Pickford et al., 2008), are associated with mitochondrial dysfunction, synaptic pathology, and morphological alterations of the Golgi apparatus in damaged AD brains, both structurally and functionally. Recent studies have provided evidence supporting the extensive involvement of autophagy in AD pathogenesis (Nixon et al., 2005; Pickford et al., 2008), which leads to the accumulation of Aβ-containing autophagic vacuoles within the dendrite of the affected neurons in AD brains (Nixon et al., 2005).

Despite of many reports on the ultrastructure of subcellular

This research was supported by Korea Basic Science Institute grant (T32404).

organelles in AD animal model and human AD patients, the correlation between Aβ plaque and other subcellular organelles, and also the interaction between subcellular organelles during AD pathogenesis remain unknown. Furthermore, the morpho-functional interaction in AD neurodegenerative disorders is still poorly understood. In this study, we examined the ultrastructural and functional alteration of subcellular organelle-related Aβ plaque and its core in the hippocampus of APP/PSEN1 double transgenic mice of the AD model.

MATERIALS AND METHODS

Animals

The seven-month-old homozygous APP/PSEN1 double transgenic mice and age-matched wild-type mice (B6C3F1/J background) were obtained from Jackson Laboratory (Bar Harbor, USA). The animal studies were performed after receiving approval of the Institutional Animal Care and Use Committee in the Korea Basic Science Institute (KBSI-ACE1013).

Immunohistochemistry

The animals were anesthetized with pentobarbital and transcardially perfused with phosphate buffered saline (PBS) and 4% paraformaldehyde at room temperature. The brains were then removed and postfixed in 4% paraformaldehyde/PBS and placed in 30% sucrose in PBS overnight at 4°C. Serial coronal sections (10 μm) were obtained with a cryostat microtome (OTF5000; Bright, Cambridge, UK) and collected on glass slides and stored at –20°C. Immunohistochemical investigations were performed according to the standard avidin-biotin-peroxidase method (Chi & Chandy, 2007). After blocking with 10% goat serum, the sections were incubated in the monoclonal anti-Aβ antibody (diluted 1:200; Abcam, Cambridge, UK) overnight at 4°C and then washed in PBS containing 0.5% bovine serum albumin. The avidin-biotin-peroxidase method with diaminobenzidine (DAB) as the chromogen was used to visualize the antibodies (brown reaction product).

Pre-embedding Immunogold Electron Microscopy

For immunogold electron microscopy (EM), the brains were fixed in 4% paraformaldehyde and 0.05% glutaraldehyde in 0.1 M phosphate buffer (pH 7.4) overnight at 4°C. Coronal sections (100 μm) were cut with a vibratome (VT1000A; Leica, Vienna, Austria) and cryoprotected in 30% sucrose overnight at 4°C. The sections were incubated with monoclonal anti-Aβ antibody (1:200; Abcam), polyclonal anti-LC3 antibody (1:200; MBL International, Woburn, MA, USA), and then incubated with 1.4 nm gold particle-conjugated secondary antibodies. The specimens were incubated with a commercially available GoldEnhance™-EM kit (Nanoprobes, New York, NY, USA) to enhance the signal from 1.4 nm gold particles. After the enhancement, samples were postfixed in 1% osmium tetroxide for 1 h, dehydrated in ethanol, and flat-embedded in Epon 812. Polymerization was conducted with pure resin at 70°C for two days. Ultrathin sections (70 nm) were obtained with an ultramicrotome (UltraCut-UCT, Leica, Austria) and then collected on Formvar-coated single-hole copper grids. After staining with 2% uranyl acetate (20 min) and lead citrate (10 min), the sections were examined using transmission electron microscopy (TEM) (Tecnai G^2 Spirit Twin; FEI, Hillsboro, OR, USA) at 120 kV.

Electron Tomography and Three-dimensional Reconstruction

The samples were sectioned in 500 nm thickness for electron tomography of the hippocampal mitochondria from wild-type and APP/PSEN1 transgenic mice. The sections placed on the Formvar-coated copper grid were stained with 2% aqueous uranyl acetate and lead citrate, and the gold particles were placed on the surface of the sections to provide fiducial points for subsequent image alignment. After carbon coating to enhance their stability in the electron beam, the sections on the grid were placed in a tilting stage and viewed using a high-voltage electron microscope (HVEM) (ARM-1300S; JEOL, Tokyo, Japan) operating at 1,250 kV. The region of interest was selected and the sample was tilted from +60° to –60° with 2° increments. A total of 61 tilt images were recorded and the digitized images were aligned using the gold particles in each tilt view as fiducial markers. The tomographic reconstruction from the tilt series was interpreted and modelled using the IMOD program package (Kremer et al., 1996). Virtual slices were extracted from the tomogram, and the boundaries of the region of interest that were visible in each tomographic slice were traced as contours overlaid on the image. The object surfaces were rendered using the AMIRA software (Visage Imaging, Carlsbad, CA, USA).

RESULTS

Detection of Aβ Plaque in the Brain of APP/PSEN1 Transgenic Mice

We prepared the brain sections from seven-month-old APP/PSEN1 transgenic mice and age-matched wild-type mice to observe the subcellular deposition of Aβ plaque. Brain sections were immunolabeled with anti-Aβ antibody and were detected by DAB immunoperoxidase reactions. We found that the circular-shaped Aβ plaques were accumulated in the hippocampus (Fig. 1A and B) and cerebral cortex (Fig. 1A and C) of the APP/PSEN1 transgenic mice brain, different from that of wild-type mice brain (Fig. 1A1).

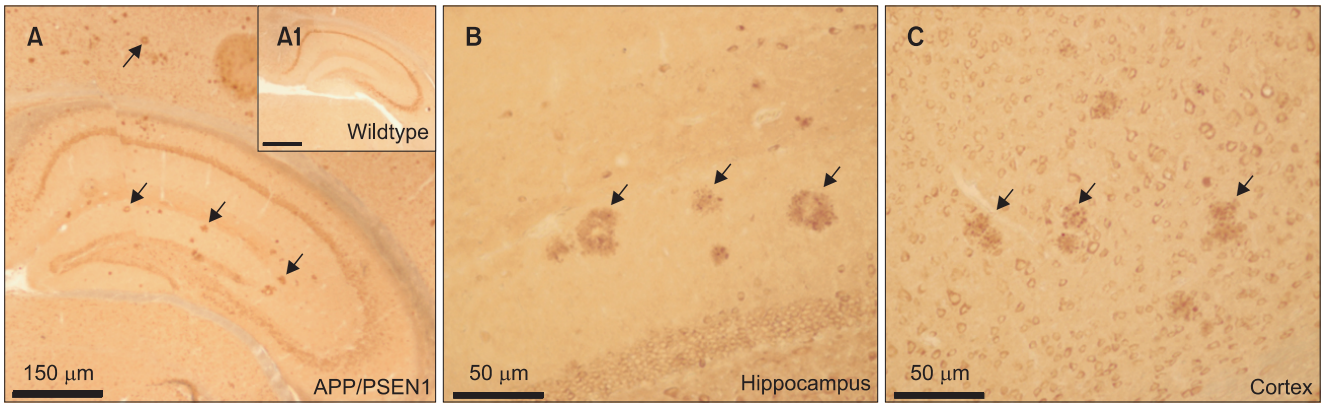

Fig. 1. Immunolabeled amyloid β (Aβ) deposits (arrows) detected in the brain of APP/PSEN1 transgenic mice. Representative images of sagittal half-brain sections taken from wild-type (A1) and APP/PSEN1 transgenic mice (A-C). Aβ plaques in the hippocampus (A, B) and cerebral cortex (A, C) of an APP/PSEN1 transgenic mice were immunolabeled with the anti-Aβ antibody and visualized with diaminobenzidine as described in Materials and Methods.

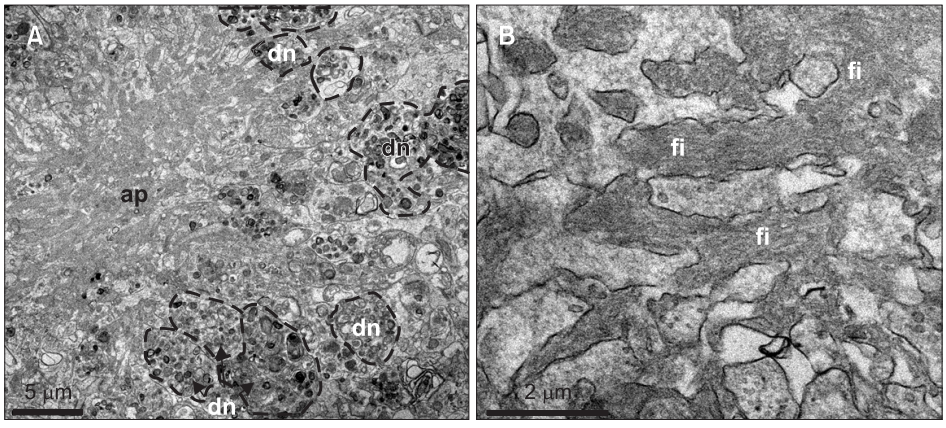

Fig. 2. Electron micrographs of amyloid β (Aβ) core in the hippocampus of APP/PSEN1 transgenic mice brain. Representative low- (A) and high- (B) magnification micrographs acquired from anti-Aβ antibody-positive Aβ plaque region in Fig. 1. ap, Aβ plaque; dn, dystrophic neurite (dotted circles in A); fi, Aβ filaments.

Ultrastructure of Amyloid Plaque and Dystrophic Neurite in the Hippocampus

Aβ-positive hippocampus regions of the APP/PSEN1 transgenic mice brain in Fig. 1 were analyzed using TEM to characterize the ultrastructural features of the Aβ plaque deposits (Fig. 2) and dystrophic neurite (Fig. 3). The ultrastructural feature of the Aβ plaque core was a star-shaped appearance with spokes of amyloid that extended outward, with a core surrounded by several dystrophic neurites (Fig. 2A). In higher-magnification images, the Aβ plaque core was compacted with an amorphous bundle structure and the Aβ filaments were accumulated in each structure (Fig. 2B).

Abnormally enlarged dystrophic neurites were filled mainly with various vesicular and membranous electron-dense structures (Fig. 3A). In high-magnification images, these vesicular structures compacted with the membranous components showing various electron densities. To identify these structures, we performed immunogold labeling with anti-LC3 antibody as an autophagosome marker. Fig. 3C shows that LC3 was labeled in this vesicular structure. Consequently, we identified the existence of autophagosomes in the dystrophic neurite of APP/PSEN1 transgenic mice. In addition, we investigated the possibility of Aβ being accumulated within the autophagosome of dystrophic neurite and confirmed the accumulation of Aβ-targeting gold particles in the autophagosome of dystrophic neurite using immunogold labeling of anti-Aβ antibody (Fig. 3D).

Morphological Alteration of Subcellular Organelles in APP/PSEN1 Transgenic Mice

We examined the synapse and myelin sheaths of axons using TEM. More disrupted myelin sheaths and synapse were found in APP/PSEN1 transgenic mice compared with the wild-type mice (Fig. 4). The myelin sheath in APP/PSEN1 transgenic mice had a frayed lamellae structure. Abnormal axons containing scarred loops of myelin flanking were found in APP/PSEN1 transgenic mice, different from that of wild-type mice (Fig. 4A). Fig. 4B represents the electron micrographs of hippocampal synapses near the Aβ deposit. Abnormal shape of presynaptic axon and dendritic spines, a shortened length

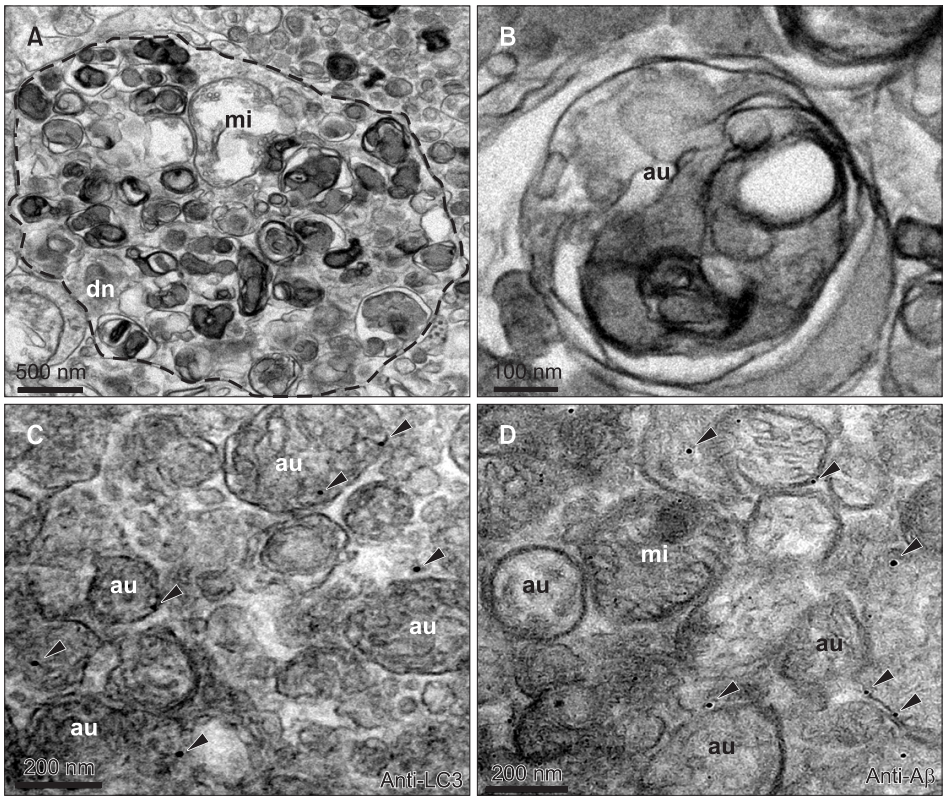

Fig. 3. Electron micrographs of dystrophic neurite in the hippocampus of APP/PSEN1 transgenic mice brain. (A) Representative micrographs of abnormally enlarged dystrophic neurite (dn, dotted circle) filled mainly with vesicular and membranous electron-dense bodies and autophagosome. (B) High-magnification micrographs of autophagosome (au) in dystrophic neurite. (C, D) Distribution of LC3 (C) and Aβ (D) in the autophagosome (au) identified by immunogold labeling using antibodies to LC3 and Aβ, respectively. All images were acquired from the anti-Aβ antibody-positive Aβ plaque region in Fig. 1. mi, mitochondria; Aβ, amyloid β.

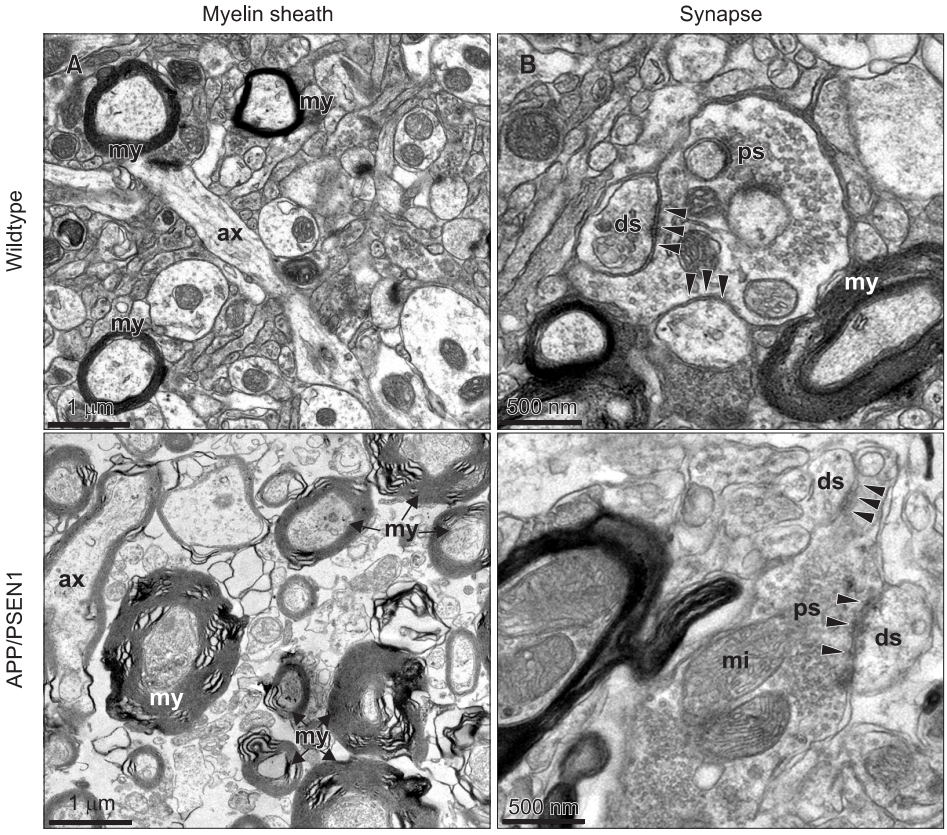

Fig. 4. Ultrastructural alteration of myelin sheaths of axon and synapse in APP/PSEN1 transgenic mice. Representative micrographs of myelin sheaths (A) and synapse (B) were acquired from wild-type mice and APP/PSEN1 transgenic mice, respectively. The redundant loops of myelin sheath (my) and the irregular gap of synaptic cleft and diffused postsynaptic density (arrowheads) were shown in APP/PSEN1 transgenic mice. ax, axon; ds, dendritic spines; ps, presynaptic axon; mi, mitochondria.

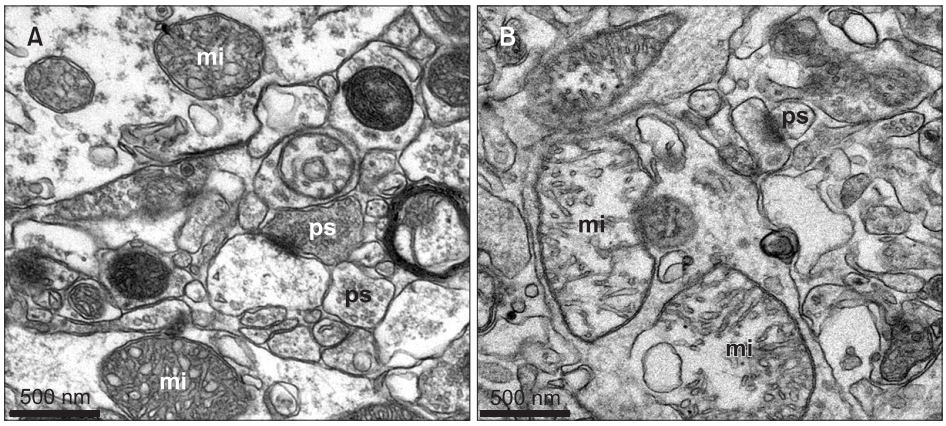

Fig. 5. Ultrastructural alteration of mitochondria in the hippocampus of APP/PSEN1 transgenic mice. Representative images taken from the hippocampus of wild-type mice (A) and APP/PSEN1 transgenic mice (B). Most of the mitochondria (mi) were swollen and the mitochondrial membrane and cristae were severely disrupted in APP/PSEN1 transgenic mice (B). ps, presynaptic axon.

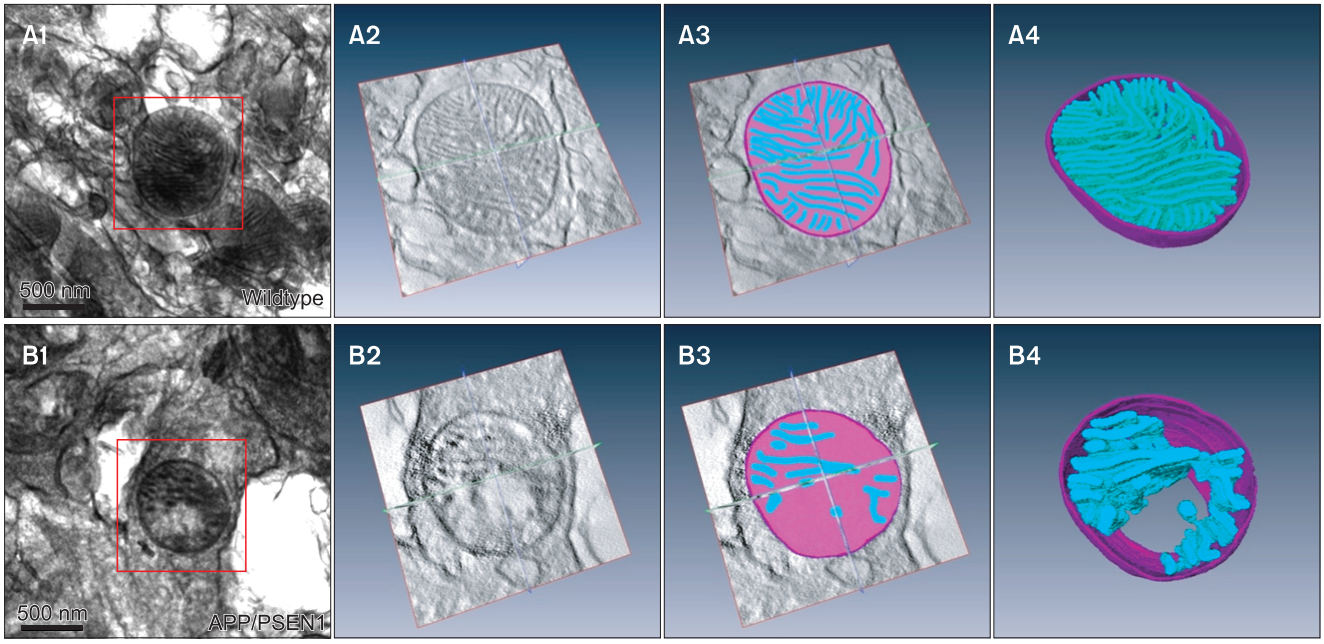

Fig. 6. Three-dimensional reconstruction of 0.5 μm-thick section of the hippocampal mitochondria from wild-type (A) and APP/PSEN1 transgenic mice (B). The tilt series containing 61 images were recorded over a tilt range of -60° to 60° with an interval of 2°. The three-dimensional model shows that most of the cristae were disrupted in the APP/PSEN1 transgenic mice. (red square box in A1, B1) The 0° image at high-voltage electron microscopy. (A2, B2) The 2.5 nm virtual digital slice extracted from the tomogram. (A3, B3) Boundaries of the region of interest that were visible in each tomographic slice were traced as contours overlaid on the image. (A4, B4) Object surfaces were rendered using the AMIRA software (Visage imaging). The mitochondrial membranes and cristae were represented as violet and cyan, respectively.

of the presynaptic active zone, irregular gap of synaptic cleft, and diffused postsynaptic density were found in APP/PSEN1 transgenic mice.

Mitochondrial alterations and dysfunction have been reported in neurodegenerative disease models including AD (Baloyannis, 2006; Umeda et al., 2011). Therefore, we focused on the functional and morphological alterations of the mitochondria in APP/PSEN1 transgenic mice. Most of the mitochondria in the hippocampus of the APP/PSEN1 transgenic mice were swollen, different from the structure found in wild-type mice (Fig. 5A). In addition, the inner mitochondrial membrane and cristae were more severely disrupted in the APP/PSEN1 transgenic mice compared with the wild-type mice (Fig. 5B). We also investigated the ultrastructural alteration of mitochondria using HVEM and three-dimensional (3D) tomography (Fig. 6). It confirmed that the mitochondrial membrane (violet in Fig. 6B4) and cristae (cyan in Fig. 6B4) in transgenic mice were severely damaged. The fragmented cristae that remained in the disrupted mitochondria were also swollen.

DISCUSSION

In this study, we investigated the ultrastructural alteration of subcellular organelles in the hippocampus of APP/PSEN1 double transgenic mice, which is a well-established transgenic mouse model of AD. However, the relationship of these abnormalities to Aβ accumulation is not yet clear. We performed an ultrastructural investigation using conventional TEM, immuno EM, and 3D tomography to clarify the effect of Aβ accumulation on the morpho-functional alteration of subcellular organelles. We confirmed the presence of Aβ plaque in the hippocampus and cerebral cortex of AD mice using immunohistochemistry (Fig. 1). Moreover, our data showed that the protein expression and ultrastructure of various subcellular organelles in the Aβ-accumulated region obviously changed.

According to recent reports, autophagy is formed in AD brain and is considered a characteristic model of AD pathology, which leads to the accumulation of autophagosomes containing Aβ peptides within the affected neurons (Nixon et al., 2005). Autophagosomes are defined by their ultrastructural characteristics and a selective association with LC3 isoform (Kabeya et al., 2000). Autophagosomes contain active enzymes such as β- and γ-secretase, which are needed to generate Aβ (Yu et al., 2004). In the present study, we observed the formation of the dystrophic neurites near the Aβ plaque core. Dystrophic neurites were filled with electron dense vesicular structures surrounded by double membranes. In addition, we confirmed the existence of autophagosomes in the dystrophic neurite and the localization of Aβ in autophagosomes by immunogold EM using anti-LC3 and anti-Aβ antibodies, respectively (Fig. 2).

In spite of various researches on the ultrastructure of autophagosomes, the structural development, especially the membrane formation mechanism, is still unknown. The membranes of endoplasmic reticulum, mitochondria, and Golgi complex were suggested to be involved in autophagosomal membrane formation. However, the participation of each membrane source in a particular stage of autophagosome formation is not yet clear (Geng & Klionsky, 2010).

The physiological role of mitochondrial Aβ could not be confirmed by direct evidence, although it has been demonstrated that Aβ is involved in mitochondrial damage (Keil et al., 2004). In AD, toxic Aβ peptides are bound with alcohol dehydrogenase in the matrix of the mitochondria and are involved in generating mitochondrial reactive oxygen species (ROS) by inhibiting the function of this enzyme (Baloyannis, 2006; Umeda et al., 2011). In addition, ROS caused further mitochondrial dysfunction, including change of membrane potential and release of cytochrome c in the cytoplasm (Manczak et al., 2006). In the present study, the inner membrane and cristae of the mitochondria in the hippocampus of APP/PSEN1 transgenic mice were severely disrupted (Figs. 5 and 6).

In normal condition, the neuronal terminals transmit information between cells to process signal transduction (Bertoni-Freddari et al., 1996). During aging, however, the number of synapses and their transmission of signals dramatically decrease (Scheff et al., 1991). According to recent studies, the expression of synaptic proteins decreases in the brain of AD patients, and the efficiency of synaptic protein involved in signal transduction through the synapse is closely associated with AD progression (Gylys et al., 2004; Almeida et al., 2005; Reddy et al., 2005; Baloyannis, 2006; Reddy & Beal, 2008). In the present study, abnormal shapes of the presynaptic axon and the dendritic spines, shortened length of the presynaptic active zone, irregular gap of the synaptic cleft, and diffused postsynaptic density were found in APP/PSEN1 transgenic mice (Fig. 4B). The results of this study suggest that the structural changes of the synaptic region are caused by Aβ that aggregated near the synapse and may contribute to the loss of signal transduction through the synapses. However, further studies are required to investigate the precise mechanisms related to Aβ-induced synaptic changes in AD pathogenesis.

CONCLUSIONS

In this study, we reported the ultrastructure of the Aβ core, change of endogenous organelle-specific protein localization, and morphological alterations of subcellular organelles, including autophagosomes, motochondria, neuronal axons and myelin, and synapses near the Aβ-deposited AD region in the hippocampus of APP/PSEN1 double transgenic mice. These basic results may be beneficial for understanding the structural changes of subcellular organelles in AD and to propose possible molecular mechanisms that are helpful to overcome neurodegenerative disorders including AD.

REFERENCES

Almeida C G, Tampellini D, Takahashi R H, Greengard P, Lin M T, Snyder E M, and Gouras G K (2005) Beta-amyloid accumulation in APP mutant neurons reduces PSD-95 and GluR1 in synapses. *Neurobiol. Dis.* **20**, 187-198.

Baloyannis S J (2006) Mitochondrial alterations in Alzheimer's disease. *J. Alzheimers. Dis.* **9**, 119-126.

Bertoni-Freddari C, Fattoretti P, Paoloni R, Caselli U, Galeazzi L, and Meier-Ruge W (1996) Synaptic structural dynamics and aging. *Gerontology.* **42**, 170-180.

Chi V and Chandy K G (2007) Immunohistochemistry: paraffin sections using the Vectastain ABC kit from vector labs. *J. Vis. Exp.* **8**, 308.

Geng J and Klionsky D J (2010) The Golgi as a potential membrane source for autophagy. *Autophagy.* **6**, 950-951.

Gylys K H, Fein J A, Yang F, Wiley D J, Miller C A, and Cole G M (2004) Synaptic changes in Alzheimer's disease: increased amyloid-beta and gliosis in surviving terminals is accompanied by decreased PSD-95 fluorescence. *Am. J. Pathol.* **165**, 1809-1817.

Kabeya Y, Mizushima N, Ueno T, Yamamoto A, Kirisako T, Noda T, Kominami E, Ohsumi Y, and Yoshimori T (2000) LC3, a mammalian homologue of yeast Apg8p, is localized in autophagosome membranes after processing. *EMBO. J.* **19**, 5720-5728.

Keil U, Bonert A, Marques C A, Scherping I, Weyermann J, Strosznajder J B, Müller-Spahn F, Haass C, Czech C, Pradier L, Müller W E, and Eckert A (2004) Amyloid beta-induced changes in nitric oxide production and mitochondrial activity lead to apoptosis. *J. Biol. Chem.* **279**, 50310-50320.

Kocherhans S, Madhusudan A, Doehner J, Breu K S, Nitsch R M, Fritschy J M, and Knuesel I (2010) Reduced Reelin expression accelerates amyloid-beta plaque formation and tau pathology in transgenic Alzheimer's disease mice. *J. Neurosci.* **30**, 9228-9240.

Kremer J R, Mastronarde D N, and McIntosh J (1996) Computer visualization of three-dimensional image data using IMOD. *J. Struct. Biol.* **116**, 71-76.

Manczak M, Anekonda T S, Henson E, Park B S, Quinn J, and Reddy P H (2006) Mitochondria are a direct site of A beta accumulation in Alzheimer's disease neurons: implications for free radical generation and oxidative damage in disease progression. *Hum. Mol. Genet.* **15**, 1437-1449.

Manczak M, Mao P, Calkins M J, Cornea A, Reddy A P, Murphy M P, Szeto H H, Park B, and Reddy P H (2010) Mitochondria-targeted antioxidants protect against Abeta toxicity in Alzheimer's disease neurons. *J. Alzheimers. Dis.* **20**, S609–S631.

Nixon R A, Wegiel J, Kumar A, Yu W H, Peterhoff C, Cataldo A, and Cuervo A M (2005) Extensive involvement of autophagy in Alzheimer disease: an immuno-electron microscopy study. *J. Neuropathol. Exp. Neurol.* **64**, 113-122.

Pickford F, Masliah E, Britschgi M, Lucin K, Narasimhan R, Jaeger P A, Small S, Spencer B, Rockenstein E, Levine B, and Wyss-Coray T (2008) The autophagy-related protein beclin 1 shows reduced expression in early Alzheimer disease and regulates amyloid beta accumulation in mice. *J. Clin. Invest.* **118**, 2190-2199.

Reddy P H (2009) Amyloid beta, mitochondrial structural and functional dynamics in Alzheimer's disease. *Exp. Neurol.* **218**, 286-292.

Reddy P H and Beal M F (2008) Amyloid beta, mitochondrial dysfunction and synaptic damage: implications for cognitive decline in aging and Alzheimer's disease. *Trends. Mol. Med.* **14**, 45-53.

Reddy P H, Mani G, Park B S, Jacques J, Murdoch G, Whetsell W Jr, Kaye J, and Manczak M (2005) Differential loss of synaptic proteins in Alzheimer's disease: implications for synaptic dysfunction. *J. Alzheimers. Dis.* **7**, 103-117.

Scheff S W, Scott S A, and DeKosky S T (1991) Quantitation of synaptic density in the septal nuclei of young and aged Fischer 344 rats. *Neurobiol. Aging.* **12**, 3-12.

Stieber A, Mourelatos Z, and Gonatas N K (1996) In Alzheimer's disease the Golgi apparatus of a population of neurons without neurofibrillary tangles is fragmented and atrophic. *Am. J. Pathol.* **148**, 415-426.

Takahashi R H, Almeida C G, Kearney P F, Yu F, Lin M T, Milner T A, and Gouras G K (2004) Oligomerization of Alzheimer's β-amyloid within processes and synapses of cultured neurons and brain. *J. Neurosci.* **24**, 3592-3599.

Umeda T, Tomiyama T, Sakama N, Tanaka S, Lambert M P, Klein W L, and Mori H (2011) Intraneuronal amyloid β oligomers cause cell death via endoplasmic reticulum stress, endosomal/lysosomal leakage, and mitochondrial dysfunction in vivo. *J. Neurosci. Res.* **89**, 1031-1042.

Yu W H, Kumar A, Peterhoff C, Shapiro Kulnane L, Uchiyama Y, Lamb B T, Cuervo A M, and Nixon R A (2004) Autophagic vacuoles are enriched in amyloid precursor protein-secretase activities: implications for beta-amyloid peptide over-production and localization in Alzheimer's disease. *Int. J. Biochem. Cell. Biol.* **36**, 2531-2540.